

Effects of ultraviolet radiation on marine primary production with reference to satellite remote sensing

Teng LI¹, Yan BAI (✉)¹, Gang LI², Xianqiang HE¹, Chen-Tung Arthur CHEN³, Kunshan GAO⁴, Dong LIU¹

¹ State Key Laboratory of Satellite Ocean Environment Dynamics, Second Institute of Oceanography, State Oceanic Administration, Hangzhou 310012, China

² Key Laboratory of Tropical Marine Bio-resources and Ecology, South China Sea Institute of Oceanology, Chinese Academy of Sciences, Guangzhou 510301, China

³ Institute of Marine Geology and Chemistry, College of Marine Sciences, National Sun Yat-Sen University, Kaohsiung 80424, Taiwan

⁴ State Key Laboratory of Marine Environmental Science, Xiamen University, Xiamen 361005, China

© Higher Education Press and Springer-Verlag Berlin Heidelberg 2014

Abstract Incubation experiments have shown that ultraviolet radiation (UVR) has significant influences on marine primary production (MPP). However, existing satellite remote sensing models of MPP only consider the effects of visible light radiation, ignoring the UVR. Additionally, the ocean color satellite data currently used for MPP estimation contain no UV bands. To better understand the mechanism of MPP model development with reference to satellite remote sensing, including UVR's effects, we first reviewed recent studies of UVR's effects on phytoplankton and MPP, which highlights the need for improved satellite remote sensing of MPP. Then, based on current MPP models using visible radiation, we discussed the quantitative methods used to implement three key model variables related to UVR: the UVR intensity at the sea surface, the attenuation of UVR in the euphotic layer, and the maximum or optimal photosynthetic rate, considering the effects of UVR. The implementation of these UVR-related variables could be useful in further assessing UVR's effects on the remote sensing of MPP, and in re-evaluating our existing knowledge of MPP estimation at large spatial scales and long-time scales related to global change.

Keywords photosynthetically active radiation, ultraviolet radiation, marine primary production, satellite remote sensing, radiative transfer model

1 Introduction

Marine primary production (MPP) is defined as the daily carbon fixation mass of phytoplankton per unit area (e.g., mg C/(m²·day)) within the euphotic layer, a layer corresponding to a penetration depth of 1% of surface radiation (Behrenfeld and Falkowski, 1997a). MPP represents the ability of phytoplankton to produce organic compounds from inorganic materials, which is the basis of the marine food chain and carbon fixation in marine ecosystems. The major environmental factors influencing MPP are light, temperature, nutrients, mixed layer depth, and the grazing of organisms such as zooplankton. Among these factors, light is a critical one as it drives photosynthesis. Light can influence the physiological activity of phytoplankton and affect photosynthetic efficiency.

In previous studies, the photosynthetically-available radiation (PAR) in remote sensing models of MPP only considered the visible light from solar radiation (400–700 nm) (Behrenfeld and Falkowski, 1997a; Campbell et al., 2002; Friedrichs et al., 2009). However, numerous studies have shown that solar ultraviolet radiation (UVR, 280–400 nm) can also significantly affect MPP (Behrenfeld, 1990; Gala and Giesy, 1991; Vincent and Roy, 1993; Helbling et al., 1994; LokaBharathi et al. 1997; Hiriart, 2000; Helbling et al., 2001; Tedetti and Sempéré, 2006; Singh et al., 2011). With the current increasing attention directed to climate change, more studies have been carried out to understand UVR's effects on MPP. A recent paper published in *Nature Climate Change* by Gao et al. (2012) showed that at the current rate of anthropogenic CO₂ emission, ocean acidification and an increase in sea surface radiation (including UVR) could reduce the carbon fixation

1 capability of phytoplankton and could lead to species
evolution of phytoplankton communities.

5 Generally, UVR can negatively inhibit the growth of
phytoplankton (Villafañe et al., 2003; Häder and Sinha,
2005), destroy photosynthetic pigments in the cells (Pang
et al., 2010), and reduce the rate of carbon fixation. For
example, the inhibitory effect of enhanced UVB on
10 phytoplankton primary productivity has been indicated in
the Southeast Pacific (Behrenfeld, 1990); and up to a 29%
reduction of surface carbon fixation by UVR has been
shown in the South China Sea (Li et al., 2011). On the
other hand, UVR can positively increase the coastal MPP
15 under low solar irradiance or strong vertical mixing
conditions (Helbling et al., 2003; Gao et al., 2007a, b; Li
and Gao, 2013). For example, Barbieri et al. (2002) found
that UVR increases the MPP of post-bloom phytoplankton
assemblies by up to 25% when the PAR irradiance was 2
W/m². Thus, the effects of UVR should be considered in
20 the estimation of satellite-derived MPP and its impact on
global MPP should be evaluated, especially for the
assessment of long-term variation in global MPP and
MPP responses to climate change.

25 Satellite remote sensing of MPP is critical for studying
the marine carbon cycle at the global scale over long time
periods. Since the successful launch of the first satellite
ocean color sensor (the Coastal Zone Color Scanner,
CZCS) in 1978, MPP estimation has been one of the main
goals of ocean color remote sensing (IOCCG, 2008).
However, the current ocean color satellites for MPP
30 estimation do not collect information in the UV bands,
with their shortest wavelength generally at 412 nm.
Moreover, the development and validation of MPP remote
sensing models has been based on field measurements,
which used phytoplankton incubated in polycarbonate or
35 glass containers, and such containers prevent the penetra-
tion of UVR (Helbling et al., 1994). Thus, the assessment
of UVR influence on the accuracy of satellite remote
sensing MPP estimation is a challenging and ongoing field
of research, which needs more field data as well as newer
40 MPP models.

This review study is intended to direct future work more
systemically toward remote sensing estimation of MPP
with the consideration of UVR's effects. In Section 2, we
review recent studies of UVR's effects on phytoplankton
and MPP. In Section 3, we discuss the temporal and spatial
45 variation of MPP under the effects of UVR, which further
highlights the need for improved satellite remote sensing
of MPP estimation. In Section 4, we review and discuss
quantitative methods used to implement three key UVR-
related variables in MPP models, namely, the UVR
50 irradiance at the sea surface, the attenuation coefficient
of UVR in the water column, and the maximum or optimal
photosynthetic rate, based on existing MPP models.
Finally, we present our summary and prospects in
55 Section 5.

2 UVR's effects on MPP

UVR has two parts, UVA (315–400 nm) and UVB (280–
315 nm). UVB photons have higher energy, and have a
5 larger influence on the biological activity of marine
phytoplankton per unit intensity compared to UVA (Cullen
et al., 1992; Wu and Gao, 2011). Based on biological
weighting functions, the inhibition of carbon fixation rate
caused by energy per unit wavelength at 280 nm (UVB) is
10 about 1 million times higher than the inhibition caused by
radiation with wavelengths longer than 320 nm (UVA)
(Wu and Gao, 2011). However, the integrated intensity of
UVA that arrives at the Earth's surface at noon is about 20
times higher than the integrated intensity of UVB. Thus,
15 UVA's impact on phytoplankton is also substantial (Wang
et al., 1999; Tedetti and Sempéré, 2006).

UVB and UVA intensities account for only 0.71%–
0.86% and 15.5%–17.8% of the visible radiation at the
ocean surface, respectively (Gao et al., 2007a). However,
20 the light at these wavelengths has more complicated effects
on phytoplankton than visible light, because of its
significantly higher photon energy. Generally, the main
factors controlling the physiological response of phyto-
plankton to UVR include the intensity of UVR, the state of
25 ocean mixing, and the composition of the phytoplankton
community (Li, 2006). Thus, we will discuss these factors
one by one.

2.1 Effects of UVR intensity

Light intensity is one of the most important factors
controlling the effects of UVR on MPP. UVR's inhibitory
35 effects on MPP generally take place under high light
conditions, although the threshold depends on the
phytoplankton species. Barbieri et al. (2002) reported
that UVR reduced the MPP of phytoplankton assemblages
collected during the bloom by around 16% when the light
40 irradiance was 66 W/m², and reduced the MPP during the
post-bloom by 13%–15% when the light intensity was
higher than 16.5 W/m². On the other hand, UVR
noticeably increased MPP when the light irradiance was
lower (Barbieri et al., 2002), and such an effect has only
45 been found in large phytoplankton species (Li and Gao,
2013). Moreover, research has shown that phytoplankton
may be capable of photosynthetic carbon fixation when
exposed to UVR alone (Gao et al., 2007b; Li and Gao,
2013). Chen and Gao (2011) studied the influence of UVR
50 on MPP at different levels of seawater acidification, and
found that UVR combined with an increase in seawater
CO₂ promoted the growth of red tide by alga (*Phaeocystis
globosa*) under low solar irradiance levels, with a daily
average light intensity of 67.8 W/m².
55

2.2 Effects of ocean mixing

Mixing in the water column can influence UVR's effects on MPP in a complex way. Mixing can change the vertical path and speed of phytoplankton in the mixed layer, which consequently affect both the quantity and quality of light received by phytoplankton. Meanwhile, mixing can also affect species composition and nutrient level in the euphotic layer, and consequently affects UVR-induced impacts (Helbling et al., 1994; Helbling et al., 2003; Li et al., 2013).

A study by Helbling et al. (1994) in the Antarctic Ocean showed that UVR improves integrated MPP under the strong mixing condition at relatively low irradiance. However, in the coastal water of the South China Sea, it was found that UVR (mainly UVA) increases MPP in well-mixed water masses with light intensities even higher than 300 W/m² (Helbling et al., 2003). In a coral reef area of the South China Sea, inhibitive effects of UVR on phytoplankton assemblage were found to be reduced in the moderately-mixed condition as compared with the stratified condition (Li et al., 2013). Some reports indicated that due to the acclimation to lower mean irradiance, the carbon fixation of phytoplankton taken from the deeper water was more vulnerable to the inhibitive effects of solar UVR than that taken from the surface water under the same light intensity (Helbling et al., 1994; Yuan et al., 2007).

Furthermore, ocean mixing can change the nutrient level in the water column, which makes UVR's effects on MPP more complicated. Many studies showed that phytoplankton are more sensitive to UVR when their habitats are nutrient limited. For example, Litchman et al. (2002) found that UVB caused more than a 1.5-fold greater additional inhibition of nitrogen-limited (N-limited) compared to N-repleted dinoflagellates. Helbling et al. (2013) reported that an increased phosphate concentration in vertically mixed water stimulates a seriously different response to UVR by phytoplankton assemblies from clear water and those from opaque water. Li and Gao (2014) observed that UVA and UVB induced 2.8% and 3.1% additional inhibitions of N-limited than N-sufficient diatoms, respectively.

2.3 Effects of phytoplankton species

UVR's effects on MPP also vary with the community structure of phytoplankton (Li et al., 2009). Microphytoplankton (> 20 µm) can synthesize UV-absorbing compounds, which can protect the cells against the damages from UVR (Garcia-Pichel, 1994; Li, 2006). In conditions with highly-varied or low-light intensity, UVA increased the carbon fixation rate of microphytoplankton from the coastal waters and thus increased MPP (Helbling et al., 2003; Gao et al., 2007b; Li et al., 2011). Wang et al. (2002) studied the UVB sensitivity of seven phytoplankton species, and found that the most sensitive species is green algae, followed by diatoms, and then by chryso-

phytes. These differences may result from variation in UV-absorbing compounds produced, and from antioxidant protection mechanisms used by phytoplankton species. Zhang et al. (2005) reported that when the UVB intensity was constant (0.0125 W/m²), a low dose of UVB improved the growth of *Alexandrium* and *Skeletonema costatum*; however, the UVB took on an inhibitory role when the dose of UVB was continuously increased. For *Heterosigma akashiwo*, however, UVB was always inhibitory.

In summary, there are many studies of UVR's effects on phytoplankton and MPP. Since the effects of UVR on MPP are closely related to the habitats of the phytoplankton, the experiments require that the target organisms are exposed to a light field as realistic to solar radiation as possible. Hence, according to the light source, the majority of these methods can be categorized as artificial radiation methods, supplemented UV-B or UVR methods, simulated in situ incubations, and in situ incubations (Villafañe et al., 2003). Outcomes from these experiments are the foundation for the development of UVR-relative MPP models. However, incubation experiments are limited in spatial and temporal variation, and need to be validated on regional and global oceans on a long term scale. More work needs to be conducted before it could be applied to the satellite remote sensing.

3 Spatial-temporal variation in UVR's effects on MPP

Spatial variation in UVR irradiance at sea surface is closely related to the spatial distributions of solar zenith angle, cloud, aerosol, and ozone in the atmosphere (Herman et al., 1999; Ahmad et al., 2003). Due to the relatively high mean solar zenith angle in the equatorial regions, the UVR intensity at the ocean surface in these areas is high all year round. However, the highest UVR irradiance at the ocean surface during the year is found in the subtropical regions where sunny weather is more frequent (Herman et al., 1999).

There are differences in the effects of UVR on MPP between the coast and open oceans. According to recent field-based studies, the phytoplankton in the open ocean suffer more UVR impacts due to its deeper penetration depth, although their cellular repair processes may have adapted to high and stable levels of UVR intensity (Tedetti and Sempéré, 2006; Villafañe et al., 2003). Experiments carried out in the South Pacific Ocean showed that the inhibitory effects of UVB on MPP were greater at high latitudes than at low latitudes (< 30°S), which might result from wide inter-species differences of phytoplankton in terms of UVB tolerance (Behrenfeld et al., 1993). In contrast, the hydrodynamic environment in the coastal ocean is complicated due to strong vertical mixing. The cell size of dominant phytoplankton species in the coastal ocean is generally larger than that in the open ocean (Li et

al., 2011); and large-size phytoplankton cells can synthesize and commutate UV-absorbing compounds (Garcia-Pichel, 1994). This can not only protect the cells from UVR damages under higher light intensity but also helps them to energize photosynthesis under relatively lower and varying light intensities, thus increasing MPP (Li, 2006; Gao et al., 2007b). However, the process of synthesizing UV-absorbing compounds could cause energy loss in phytoplankton cells, which is unfavorable for their growth and reproduction (Calkins and Thordardottir, 1980). Overall, the effects of UVR on MPP in the coastal ocean may be much more complicated than in the open ocean.

In addition to spatial variation, there is temporal variation in UVR's effects on MPP, including seasonal, inter-annual, and long-term changes. Due to the seasonal changes of the solar incidence and ozone content in the atmosphere, there is strong seasonal variation in UVR intensity at the sea surface (Frederick et al., 1989; Herman et al., 1999). The underwater transmission of UVR also varies with season due to the seasonal variations in water turbidity. Moreover, phytoplankton species may also vary with season due to the change in nutrient level induced by mixing or riverine input, which results in seasonal variation in the sensitivity of phytoplankton to UVR (Wu et al., 2010; Mizubayashi et al., 2013).

For a global warming scenario over a long time scale, the UVR intensity at sea surface is likely to increase due to the decline of the stratosphere ozone layer (Madronich et al., 1998), or decrease due to the increase of cloud cover (He et al., 2013). Global warming could also decrease the mixed layer depth (Huot et al., 2000) and may enhance UVR's impacts on MPP, especially in the area under ozone hole (Helbling et al., 1994). Biologically-oriented research initiated in 1987 into the impacts of UVR on Antarctic phytoplankton showed that primary production rates decreased due to the effects of UVR, particularly due to the shorter wavelengths of UVR (El-Sayed et al., 1990). Thus, long-term monitoring of the effects of UVR on MPP on a global scale is necessary (Behrenfeld et al., 1993), and observations from satellite remote sensing could be used as a very powerful tool.

4 Satellite remote sensing of MPP considering UVR's effects

4.1 Principle of remote sensing models of MPP

The main objective of MPP estimation by remote sensing is to establish the relationship between MPP and the factors that influence phytoplankton photosynthesis. So far, several MPP models using visible PAR have been reviewed (Behrenfeld and Falkowski, 1997a; Campbell et al., 2002; Carr et al., 2006). Here, we briefly discuss the general principle of MPP models as a foundation for further discussion on the development of MPP models that

include UVR's effects.

The early empirical MPP models were established through simple statistical regression between in situ MPP and chlorophyll *a* (*chl*_a) concentration (Lorenzen, 1970; Eppley et al., 1985). With increasing knowledge of the physiological processes of phytoplankton photosynthesis, more analytical models of MPP were proposed, which took factors such as biomass and photosynthetically available radiance (PAR) into account, along with transfer or yield functions that described physiological responses of the measured *chl*_a to light, nutrients, temperature, and other environmental variables. Some models included vertical distributions of these properties within the euphotic layer (Campbell et al., 2002; Carr et al., 2006). However, there have been no truly analytical models to date; all extant models depend on empirical parameterizations to some extent (Carr et al., 2006).

Based on implicit levels of mathematical integration, Behrenfeld and Falkowski (1997a) classified MPP models into four groups (Table 1), namely, wavelength-resolved models (WRM), wavelength-integrated models (WIM), time-integrated models (TIM), and depth-integrated models (DIM). All of these models include contributions from depth-integrated primary production, surface phytoplankton biomass, photo-adaptivity, euphotic depth, and irradiance-dependence (Behrenfeld and Falkowski, 1997a). The widely used vertically generalized production model (VGPM) is a depth-integrated model, in which PAR has a relatively minor effect on MPP variability (Behrenfeld and Falkowski, 1997b). However, for MPP models based on the photosynthesis vs. irradiance response curve (PvsE curve) and wavelength-resolved or wavelength-integrated models, PAR has a significant effect on MPP (Carr et al., 2006).

In addition to the classification defined by Behrenfeld and Falkowski (1997a), there is another kind of classification based on phytoplankton mass, namely, the chlorophyll-based model (Chl-bPM), which includes pigment concentration (Marra et al., 2003), phytoplankton absorption-based model (AbPM) (Lee et al., 1996; Marra et al., 2003; Hirawake et al., 2011), and phytoplankton carbon-based model (CbPM) (Behrenfeld et al., 2005) (Table 1). The differences between these models are in the expression of biomass and its corresponding physiological variables. The majority of the models in Behrenfeld and Falkowski's (1997a) classification system are chlorophyll-based. Rather than using the concentration of *chl*_a or photosynthetic pigments as the core of an MPP model, phytoplankton absorption based models (AbPM) concentrate on the quantum yield rate of photosynthesis, which can reduce uncertainties from satellite-derived *chl*_a estimation and the bias in sea surface temperature-derived values of the optimal photosynthetic rate of *chl*_a-normalized productivity (Hirawake et al., 2011). Instead of relating MPP to *chl*_a and the maximum or optimal photosynthetic rate, phytoplankton carbon-based model (CbPM) relates MPP to

Table 1 Typical MPP models of satellite remote sensing

Types*	Normal formula	Source
WRM	$PP = \int_{\lambda=400nm}^{\lambda=700nm} \int_{z=0}^{z=z_{eu}} \int_{t=sunrise}^{t=sunset} PAR(\lambda, t, z) \times Chla(z) \times a^*(\lambda, z) \times \phi(\lambda, t, z) d\lambda dt dz - R$	
WIM	$PP = \int_{z=0}^{z=z_{eu}} \int_{t=sunrise}^{t=sunset} PAR(t, z) \times Chla(z) \times \phi(t, z) dt dz - R$	Behrenfeld and Falkowski (1997a)
TIM	$PP = \int_{z=0}^{z=z_{eu}} PAR(z) \times Chla(z) \times P^b(z) dz$	
DIM	$PP = f[PAR(0)] \times Chla \times P_{opt}^b \times DL \times Z_{eu}$	
VGPM	$PP = [0.66125 \times PAR(0) / (PAR(0) + 4.1)] \times Chla \times P_{opt}^b \times DL \times Z_{eu}$	Behrenfeld and Falkowski (1997b)
AbPM	$PP = \int_{z=0}^{z=z_{eu}} PAR(0) \times a_{ph}(z) \times \phi(z) dz$	Marra et al., (2003)
CbPM	$PP = [PAR(0) / (PAR(0) + 4.1)] \times C_{phyto} \times u \times Z_{eu}$	Behrenfeld et al., (2005)

* Abbreviation of each model can be found in the main text. PP is the daily primary production within the euphotic layer; R is the respiration of phytoplankton; PAR is the solar irradiance, where $PAR(0)$ is the value at ocean surface and $PAR(z)$ is the value at depth z ; $chla$ is the chlorophyll a concentration; C_{phyto} is the carbon biomass of phytoplankton; a^* is the chlorophyll-specific absorption coefficient; a_{ph} is the absorption coefficient by phytoplankton; ϕ is the quantum yield of photosynthesis; P_{opt}^b is the maximum carbon fixation rate of phytoplankton; $P^b(z)$ is the carbon fixation rate of phytoplankton at depth z ; u is the phytoplankton growth rate; z_{eu} is the euphotic depth; and DL is the length of the day.

phytoplankton carbon biomass and phytoplankton growth rate, which removes the need for parameterizing the maximum or optimal photosynthetic rate with an empirical temperature-dependent function or a globally parameterized scheme of biogeochemical provinces (Behrenfeld et al., 2005). Nonetheless, phytoplankton carbon biomass and growth rate must still be estimated from a satellite-derived chlorophyll-to-carbon ratio, which has highly dynamic variation and is species-dependent. These simplifications in modeling will naturally result in uncertainties.

To date, there have been four runs of the primary production algorithm round robin (PPARR) to determine the accuracy of MPP models for predicting depth-integrated primary production. According to the results of the second and third PPARR (Campbell et al., 2002; Carr et al., 2006), the performance of MPP models was independent of the algorithms' complexity, and instead largely depended on the accuracy of model input data, especially the parameterization of the maximum or optimal photosynthetic rate. Therefore, Carr et al. (2006) suggested that any further progress in MPP modeling required an improved understanding of the effect of temperature on photosynthesis, especially in diverse regions, for a global estimation and better parameterization of the maximum photosynthetic rate.

4.2 Retrieval of UVR-related variables involved in MPP remote sensing models

Recall that the existing MPP models mostly use the PAR of visible light (e.g., 400–700 nm), and seldom consider

UVR. Therefore, we must re-evaluate MPP estimation at large scales by satellite remote sensing. This is challenging because the current ocean color data used for MPP estimation contains no information in the UV bands. As such, the retrieval of UVR information is critical for new estimation of MPP, which considers the effects of UVR. Since the MPP models structured for satellite remote sensing using the visible PAR have been widely tested, in the following sections we only discuss the quantitative methods used to implement three key variables in the MPP models, which are affected by UVR, namely, the UVR irradiance at the sea surface (E_{UVR}), the attenuation coefficient of UVR (k_{UVR}) in the water column, and the maximum or optimal photosynthetic rate (P_{opt}^b). Figure 1 shows the sketch of quantitative implementation of these three UVR-related key variables.

4.2.1 Estimation of UVR irradiance at sea surface (E_{UVR})

Before arriving at the sea surface, solar radiation is subjected to scattering and absorption in the atmosphere by air molecules, water vapor, ozone, aerosols, and clouds. Among them, ozone is primarily responsible for the absorption of UVR. Attenuation of UVR in the atmosphere is closely related to the radiation's wavelength. Scattering by atmospheric molecules and aerosols is greater for UVB than for UVA (Guo et al., 2002); moreover, UVB is strongly absorbed by ozone and the UVB irradiance reaching the Earth surface accounts for less than 1% of the total solar irradiance (Pang et al., 2010).

In addition to direct field measurements, satellite remote sensing is an important way of monitoring UVR in real-

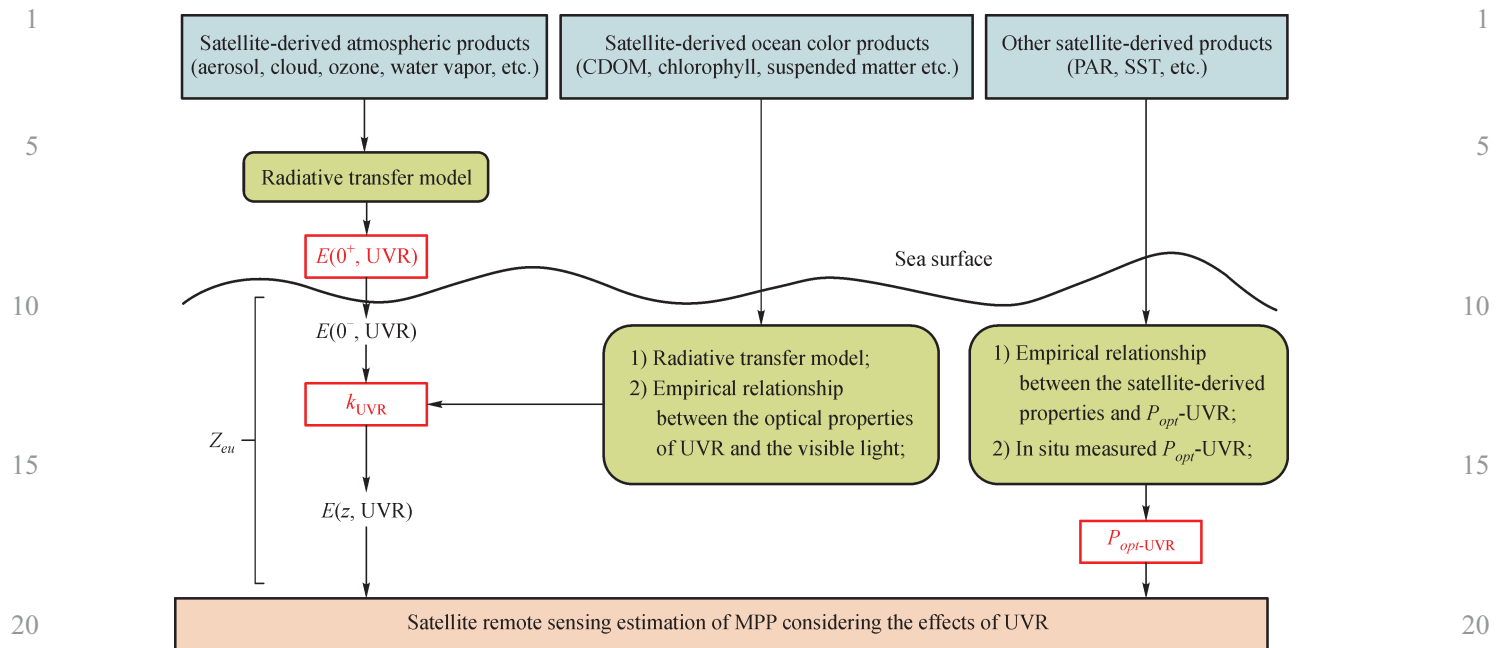


Fig. 1 A sketch of the quantitative implementation of three key UVR-related variables (shown in red color) in MPP models. The boxes in green color show the current methods used in the literature (seen in Section 4.2); boxes in light blue are the relative satellite products which can be used as model inputs.

time. However, the ocean color satellites currently used for MPP remote sensing provide no information in the UV bands, with 412 nm being the shortest wavelength detected. Thus, UVR information is usually inferred from atmospheric satellites. The first satellite that measured UVR on the Earth's surface was the Nimbus-4, which was launched by NASA in 1970. The Solar Backscatter Ultraviolet Spectrometer sensor (SBUV) onboard the Nimbus-4 had 12 channels in the UVR range (250–339.8 nm), designed to retrieve the vertical profile of ozone in the atmosphere. Its successors, the Total Ozone Mapping Spectrometer (TOMS) onboard the Nimbus-7 and the Ozone Monitoring Instrument (OMI) onboard the Aura satellite were launched in 1978 and 2002, respectively. The UVR intensity data retrieved by the TOMS is the daily erythemal dose, whereas the OMI detects the spectral UV irradiance at four separate wavelengths (305 nm, 310 nm, 324 nm, and 380 nm) during the satellite's transit time (near 1:30 PM at local time) (Tanskanen et al., 2006). Although the sensors using UVR channels are mainly designed to monitor the variation of ozone in the atmosphere, they can also be used to study the effects of UVR on Earth surface ecology. Using the water Inherent Optical Properties (IOP) data from the Sea-viewing Wide Field of View Sensor (SeaWiFS), Vasilkov et al. (2001) studied the transmission of UVR in seawater and measured destructive effects of UVR on the DNA of phytoplankton using the UVR data from the TOMS. Currently, the OMI can only measure the surface intensity of UVR at the satellite's transit time,

which cannot fully satisfy the requirement of daily irradiance for MPP estimation.

The atmospheric radiative transfer model can simulate the transmission of UVR in the atmosphere, and can provide a good estimation of the UVR intensity at the Earth's surface. For example, Brühl and Crutzen (1989) used a two-stream radiative transfer model to calculate the transmission of UVR. Based on the Discrete Ordinates Radiative Transfer model (DISORT) for the atmosphere (Jin and Stamnes, 1994), Jin et al. (2006) developed a Coupled Ocean and Atmosphere Radiative Transfer (COART) model, which can be used to simulate the transferring process of solar radiation in the atmosphere as well as in the ocean, with wavelengths from 200 nm to 100 μm . Combining an atmospheric radiative transfer model with satellite-derived atmospheric data was a feasible method for estimating UVR irradiance at the sea surface (Herman et al., 1999; Vasilkov et al., 2001; Smyth, 2011). Based on a radiative transfer model, the global maps of monthly-mean integrated UV erythemal irradiance (290–400 nm) at the Earth's surface were estimated using the atmospheric information retrieved by the TOMS (Herman et al., 1999). To improve computation efficiency, Ahmad et al. (2003) established a look-up table of surface UVR intensity under different solar zenith angles, aerosol optical thicknesses, ozone concentrations, and cloud reflectivity using a radiative transfer model. Based on the look-up table, they estimated the surface UVR irradiance at the satellite's transit time of the Nimbus 7/TOMS. Similarly, Smyth (2011) retrieved the sea surface UVR intensity at

noon through a look-up table, and further estimated the daily UV dose at four individual wavelengths (305 nm, 325 nm, 340 nm, and 380 nm) by assuming that the intensity of UVR changes following a sine function during the day. Recently, we have developed a look-up table of wavelength-integrated UVR irradiance using the COART model, which considers the variation in solar zenith angle, aerosol optical thickness at 550 nm, ozone amount, liquid water path, and total precipitable water (manuscript under preparation); and because all of the inputs for the look-up table can be obtained from satellite remote sensing, we can achieve near real-time monitoring of daily wavelength-integrated UVR for MPP estimation.

4.2.2 Estimation of UVR attenuation in seawater (k_{UVR})

As mentioned in Section 4.1, MPP is calculated by integrating the daily carbon fixation of phytoplankton within the euphotic layer. Thus, vertical distributions of relative properties in the water column are needed for calculating MPP. One of the considerations is the underwater transmission of UVR irradiance, which is determined by the optical properties of various components, including pure water, particles, and color dissolved organic matter (CDOM). Combining scattering and absorption in the water, the attenuation coefficient of seawater is a key variable that quantitatively describes the variation of radiation in the water, which changes substantially with wavelength. It is well known that UVR attenuates more rapidly than visible light, and that UVB attenuates more rapidly than UVA due to its higher absorption by water molecules and CDOM (Li, 2006; Gao et al., 2007b; Tedetti et al., 2007).

Traditionally, the diffuse attenuation coefficient of PAR at visible wavelengths (k_{PAR}) is used in the estimation of MPP. In some cases, k_{PAR} was used to estimate the depth of the euphotic layer (Barber et al., 1997; Lee et al., 2007). k_{PAR} is a wavelength-integrated and depth-dependent value, which is calculated using the PAR profile. For simplicity, the depth-averaged k_{PAR} was used to characterize the attenuation of PAR in the whole euphotic layer (Lee et al., 2005; Lee, 2009). However, the depth-averaged k_{PAR} ignores the variation in the PAR spectrum, the response of phytoplankton to different wavelengths and the variation of k_{PAR} with depth. The diffuse attenuation coefficient of UVR (k_{UVR}) is also needed for obtaining the full UVR profile in the water column when studying the effects of UVR on MPP (Booth and Morrow, 1997).

Generally, two methods are used to estimate k_{UVR} . One is to establish the relationship between k_{UVR} and k_{PAR} . For example, Højerslev and Aas (1991) found that there was a good linear relationship between the diffuse attenuation coefficients at 310 nm and 450 nm. More recently, Smyth (2011) established empirical relationships between the absorption coefficient at 443 nm and the downward

attenuation coefficient of UVR at 305 nm, 325 nm, 340 nm, and 380 nm. The other method is based on a complex underwater radiative transfer model, taking into account the absorption and scattering properties of different water components (Vasilkov et al., 2001, 2005). Vasilkov et al. (2001) calculated the radiative transfer process in the ocean using the Quasi-Single Scattering Approximation (QSSA) method that was a fast computational model allowing the estimation of UVR penetration into the water column on a global scale. To improve the accuracy of the process, Vasilkov et al. (2005) generated a look-up table based on chlorophyll *a* concentration using the radiative transfer theory to calculate the underwater UVR irradiance. Up to now, although there are a few studies on k_{UVR} , radiative transfer models containing UVR may make it possible to estimate the underwater profile of UVR using ocean color satellite data.

4.2.3 Parameterization of carbon fixation rate with the effects of UVR (P_{opt}^b)

To date, the inversion of maximum or optimal photosynthetic rate (P_{opt}^b) has been largely based on sea surface temperature or radiation intensity (Megard, 1972; Behrenfeld and Falkowski, 1997b; Ishizaka et al., 2007). However, there are a few studies on the parameterization of P_{opt}^b with UVR's effects ($P_{opt-UVR}$).

Empirical relationships between the intensity of UVR and the effects of UVR on MPP have been developed based on field measurements. By analyzing in situ data from the South Pacific, Behrenfeld et al. (1993) found that the inhibitive effect of UVB on MPP was a linear function of UVB dose. Li et al. (2011) refitted the MPP model of Eilers and Peeters (1988) using in situ data from the South China Sea, and established a model for the estimation of phytoplankton carbon fixation rate, which contains the effects of UVR.

They found that UVR could decrease sea surface primary production by 20.8% in coastal waters and by 26.7% in offshore waters.

Based on the effects of UVR on phytoplankton, biological weighted function models have been developed to estimate the effects of UVR on phytoplankton carbon fixation rate (Cullen et al., 1992; Neale et al., 1998; Yuan et al., 2007):

$$P^B = P_s^B (1 - e^{-E_{PAR}/E_s}) \left(\frac{1}{1 + E_{inh}^*} \right) \quad (1)$$

$$E_{inh}^* = \bar{e}_{PAR} E_{PAR} + \sum_{\lambda=280nm}^{400nm} \varepsilon(\lambda) E(\lambda) \Delta\lambda \quad (2)$$

where P^B is the carbon fixation rate; E_{inh}^* is the inhibitive effect of radiation on phytoplankton production; P_s^B is the

1 maximum carbon fixation rate; E_{PAR} and E_S represent the
intensity of instant PAR and that of PAR when photo-
synthesis is at saturation, respectively; $E(\lambda)$ is the radiation
irradiance at the band of λ ; $\bar{\epsilon}_{\text{PAR}}$ is the average influence of
5 PAR on phytoplankton; and $\epsilon(\lambda)$ is the effect of UVR on
phytoplankton production.

On the basis of the biological weighted function model,
Yuan et al. (2007) established a model of E_{inh}^* to describe
vertical variation in the effects of UVB on MPP by
10 defining the attenuation coefficient of E_{inh}^* in the euphotic
layer, and found that the inhibitive rate of UVB on
phytoplankton in lower layers was higher than that in
surface layer. Although the biological weighted function
model could accurately describe the influence of UVR on
15 MPP, it requires more in situ data.

5 Summary and prospects

20 The influence of UVR on MPP involves complex
photosynthetic processes, and is modulated by many
other factors. To date, most studies have been based on
field data taken from limited stations in short duration
experiments. There are a few MPP models that incorporate
25 UVR's effects, but the effects of UVR on the accuracy of
existing satellite-derived MPP measurements remain
poorly understood. Based on reviews of recent studies
regarding UVR's effects on MPP and existing remote
sensing models of MPP, we discussed quantitative methods
30 used to implement three UVR-related key variables.

Due to the lack of information on UV bands in the
current ocean color satellite sensors, a feasible way to
gather the information could be to combine satellite-
derived atmospheric information with an atmospheric
radiative transfer model to estimate the UVR irradiance
35 at sea surface (Herman et al., 1999; Vasilkov et al., 2001;
Smyth, 2011). Similarly, for the attenuation of UVR in
water column, an ocean radiative transfer model can be
combined with the ocean optical properties derived from
ocean color data (Vasilkov et al., 2001, 2005). The
40 parameterization of the maximum or optimal photosyn-
thetic rate from remote sensing is the most critical and
challenging issue in MPP modeling (Behrenfeld and
Falkowski, 1997a; Carr et al., 2006). However, due to
the complexity of UVR's effects on phytoplankton carbon
45 fixation, no analytical models of the maximum or optimal
photosynthetic rate considering UVR's effects have been
developed yet, and more efforts are needed with adequate
in situ data.

Overall, photosynthesis of phytoplankton and marine
primary production are influenced by both visible light and
UVR. The development of an MPP model for satellite
remote sensing that considers UVR is still at an early stage.
One way to re-evaluate MPP with the consideration of
55 UVR would be to replace key variables in an existing MPP

model with those UVR-related variables, and consider
their significance carefully. By doing this, we still cannot
provide a new MPP model, but we could provide some
assessments of UVR's effects on MPP estimation, to some
extent, in the first stage. To implement the suggestions for
5 MPP model improvement raised by the PPARR3 (Carr et
al., 2006), more in situ data are required, ideally combined
with ancillary data such as nutrients and community
structure. Specific concerns for future progress include the
improved formulations of the quantum yield and of the
10 light field, and more data on the vertical distribution of
chlorophyll. At the global scale and in the context of long-
term change, the effects of UVR on the estimation of MPP
should not be ignored, but the significance of UVR's
effects still needs to be carefully assessed. For the next
15 generation of ocean color satellite missions, information in
the UV bands will be available with higher signal-to-noise
ratio than that in the current atmospheric satellite data. For
example, the Pre-Aerosol, Clouds, and ocean Ecosystem
(PACE) mission by NASA, which is planned to be
20 launched around 2020, has three UV bands at 350 nm,
360 nm, and 380 nm. The next-generation Chinese ocean
color satellites of HY-1C and HY-1D will have two UV
bands at 355 nm and 385 nm. Those UV bands can be
useful for the estimations of UVR's distribution in
25 seawater and primary production.

Acknowledgements This study was supported by the National Basic
Research Program of China (No. 2009CB421202), the Public Science and
Technology Research Funds Projects for Ocean Research (No. 200905012),
the National Natural Science Foundation of China (Nos. 41322039,
41271378, and 41321004), the National Key Technology Support Program
(Nos. 2013BAD13B01 and 2012BAH32B01) and the "Global Change and
Air-Sea Interaction" project of China (No.GASI-03-03-01-01). We thank
three anonymous reviewers for their constructive comments, which
significantly strengthened the manuscript.

References

- Ahmad Z, Herman J R, Vasilkov A P, Tzortziou M, Mitchell B G, Kahru
M (2003). Seasonal variation of UV radiation in the ocean under clear
and cloudy conditions. *International Society for Optics and
Photonics, In Optical Science and Technology, SPIE's 48th Annual
Meeting*, 63–73
- Barber R T, Borden L, Johnson Z, Marra J, Knudson C, Trees C C
(1997). Ground truthing modeled-kPAR and on-deck primary
productivity incubations with in-situ observations. *Ocean Optics,
XIII. International Society for Optics and Photonics*, 834–839
- Barbieri E S, Villafañe V E, Helbling E W (2002). Experimental
assessment of UV effects on temperate marine phytoplankton when
50 exposed to variable radiation regimes. *Limnol Oceanogr*, 47(6):
1648–1655
- Behrenfeld M J (1990). Primary productivity in the Southeast Ocean:
effects of Enhanced Ultraviolet-B radiation. Thesis for the Degree of
Master of Science. Oregon State University
- Behrenfeld M J, Boss E, Siegel D A, Shea D M (2005). Carbon-based
55

- ocean productivity and phytoplankton physiology from space. *Global Biogeochem Cycles*, 19(1)
- Behrenfeld M J, Falkowski P G (1997a). A consumer's guide to phytoplankton primary productivity models. *Limnol Oceanogr*, 42 (7): 1479–1491
- Behrenfeld M J, Falkowski P G (1997b). Photosynthetic rates derived from satellite-based chlorophyll concentration. *Limnol Oceanogr*, 42 (1): 1–20
- Behrenfeld M J, Hardy J T, Gucinski H, Hanneman A, Lee H II, Wones A (1993). Effects of ultraviolet-B radiation on primary production along latitudinal transects in the South Pacific Ocean. *Mar Environ Res*, 35(4): 349–363
- Booth C R, Morrow J H (1997). The penetration of UV into natural waters. *Photochem Photobiol*, 65(2): 254–257
- Brühl C H, Crutzen P J (1989). On the disproportionate role of tropospheric ozone as a filter against solar UV-B radiation. *Geophys Res Lett*, 16(7): 703–706
- Calkins J, Thordardottir T (1980). The ecological significance of solar UV radiation on aquatic organisms. *Nature*, 283(5747): 563–566
- Campbell J, Antoine D, Armstrong R, Arrigo K, Balch W, Barber R, Behrenfeld M, Bidigare R, Bishop J, Carr M E, Esaias W, Falkowski P, Hoepffner N, Iverson R, Kiefer D, Lohrenz S, Marra J, Morel A, Ryan J, Vedernikov V, Waters K, Yentsch C, Yoder J (2002). Comparison of algorithms for estimating ocean primary production from surface chlorophyll, temperature, and irradiance. *Global Biogeochemical Cycles*, 16(3): 9–1–9–15
- Carr M E, Friedrichs M A M, Schmeltz M, Noguchi Aita M, Antoine D, Arrigo K R, Asanuma I, Aumont O, Barber R, Behrenfeld M, Bidigare R, Buitenhuis E T, Campbell J, Ciotti A, Dierssen H, Dowell M, Dunne J, Esaias W, Gentili B, Gregg W, Groom S, Hoepffner N, Ishizaka J, Kameda T, Le Quércé C, Lohrenz S, Marra J, Mélin F, Moore K, Morel A, Reddy T E, Ryan J, Scardi M, Smyth T, Turpie K, Tilstone G, Waters K, Yamanaka Y (2006). A comparison of global estimates of marine primary production from ocean color. *Deep Sea Res Part II Top Stud Oceanogr*, 53(5–7): 741–770
- Chen S W, Gao K S (2011). Solar ultraviolet radiation and CO₂-induced ocean acidification interacts to influence the photosynthetic performance of the red tide alga *Phaeocystis globosa* (Prymnesiophyceae). *Hydrobiologia*, 675(1): 105–117
- Cullen J J, Neale P J, Lesser M P (1992). Biological weighting function for the inhibition of phytoplankton photosynthesis by ultraviolet radiation. *Science*, 258(5082): 646–650
- El-Sayed S Z, Stephens F C, Bidigare R R, Ondrusek M E (1990). Effect of ultraviolet radiation on Antarctic marine phytoplankton. In: Kerry K R, Hempel G eds. *Antarctic Ecosystems*. 1st ed. Berlin-Heidelberg: Springer, 379–385
- Eppley R W, Stewart E, Abbott M R, Heyman U (1985). Estimating ocean primary production from satellite chlorophyll. Introduction to regional differences and statistics for the Southern California Bight. *J Plankton Res*, 7(1): 57–70
- Frederick J E, Snell H E, Haywood E K (1989). Solar ultraviolet radiation at the earth's surface. *Photochem Photobiol*, 50(4): 443–450
- Friedrichs M A M, Carr M E, Barber R T, Scardi M, Antoine D, Armstrong R A, Asanuma I, Behrenfeld M J, Buitenhuis E T, Chai F, Christian J R, Ciotti A M, Doney S C, Dowell M, Dunne J, Gentili B, Gregg W, Hoepffner N, Ishizaka J, Kameda T, Lima I, Marra J, Mélin F, Moore J K, Morel A, O'Malley R T, O'Reilly J, Saba V S, Schmeltz M, Smyth T J, Tjiputra J, Waters K, Westberry T K, Winguth A (2009). Assessing the uncertainties of model estimates of primary productivity in the tropical Pacific Ocean. *J Mar Syst*, 76(1–2): 113–133
- Gala W R, Giesy J P (1991). Effects of ultraviolet radiation on the primary production of natural phytoplankton assemblages in Lake Michigan. *Ecotoxicol Environ Saf*, 22(3): 345–361
- Gao K S, Li G, Helbling E W, Villafañe V E (2007a). Variability of the UVR effects on photosynthesis of summer phytoplankton assemblages from a tropical coastal area of the South China Sea. *Photochem Photobiol*, 83(4): 802–809
- Gao K S, Wu Y P, Li G, Wu H Y, Villafañe V E, Helbling E W (2007b). Solar UV Radiation drives CO₂ fixation in marine phytoplankton: a double-edged sword. *Plant Physiol*, 144(1): 54–59
- Gao K S, Xu J T, Gao G, Li Y, Hutchins D A, Huang B Q, Wang L, Zheng Y, Jin P, Cai X N, Häder D P, Li W, Xu K, Liu N N, Riebesell U (2012). Rising CO₂ and increased light exposure synergistically reduce marine primary productivity. *Nature Climate Change*, 2(7): 519–523
- Garcia-Pichel F (1994). A model for internal self-shading in planktonic organisms and its implications for the usefulness of ultraviolet sunscreen. *Limnol Oceanogr*, 39(7): 1704–1717
- Guo S C, Qin Y, Zhao B L, Wu J, Chen H, Chen Y, Qin F (2002). The research of the effects of the atmosphere to the ultraviolet radiation. *Universitatis Pekinensis*, 38(3): 334–341 (*Acta Scientiarum Naturalium*)
- Häder D P, Sinha R P (2005). Solar ultraviolet radiation-induced DNA damage in aquatic organisms: potential environmental impact. *Mutation Research/Fundamental and Molecular Mechanisms of Mutagenesis*, 571(1–2): 221–233
- He X Q, Bai Y, Pan D L, Chen C T, Chen Q, Wang D F, Gong F (2013). Satellite views of seasonal and inter-annual variability of phytoplankton blooms in the eastern China seas over the past 14 yr (1998–2011). *Biogeosciences*, 10(7): 4721–4739
- Helbling E W, Buma A G, de Boer M K, Villafañe V E (2001). In situ impact of solar ultraviolet radiation on photosynthesis and DNA in temperate marine phytoplankton. *Mar Ecol Prog Ser*, 211: 43–49
- Helbling E W, Carrillo P, Medina-Sánchez J M, Durán C, Herrera G, Villar-Argaiz M, Villafañe V E (2013). Interactive effects of vertical mixing, nutrients and ultraviolet radiation: In situ photosynthetic responses of phytoplankton from high mountain lakes in Southern Europe. *Biogeosciences*, 10(2): 1037–1050
- Helbling E W, Gao K S, Gonçalves R J, Wu H, Villafañe V E (2003). Utilization of solar UV radiation by coastal phytoplankton assemblages off SE China when exposed to fast mixing. *Mar Ecol Prog Ser*, 259: 59–66
- Helbling E W, Villafañe V E, Holm-Hansen O (1994). Effects of ultraviolet radiation on Antarctic marine phytoplankton photosynthesis with particular attention to the influence of mixing. *Antarct Res Ser*, 62: 207–227
- Herman J R, Krotkov N, Celarier E, Larko G D, Labow G (1999). Distribution of UV radiation at the earth's surface from TOMS-measured UV-backscattered radiances. *J Geophys Res*, D, Atmospheres, 104(D10): 12059–12076
- Hirawake T, Takao S, Horimoto N, Ishimaru T, Yamaguchi Y, Fukuchi

- M (2011). A phytoplankton absorption-based primary productivity model for remote sensing in the Southern Ocean. *Polar Biol*, 34(2): 291–302
- Hiriart V P (2000). Ultraviolet radiation and primary production by Lake Erie phytoplankton communities. University of Waterloo
- Højerslev N, Aas E (1991). A relationship for the penetration of ultraviolet B radiation into the Norwegian Sea. *J Geophys Res*, 96 (C9): 17003–17005
- Huot Y, Jeffrey W H, Davis R F, Cullen J J (2000). Damage to DNA in Bacterioplankton: A model of damage by ultraviolet radiation and its repair as influenced by vertical mixing. *Photochem Photobiol*, 72(1): 62–74
- IOCCG (2008). Why ocean colour? The societal benefits of ocean-colour technology. In: Platt T, Hoepffner N, Stuart V, Brown C, eds. Reports of the international ocean-colour coordinating group, No.7, IOCCG, Dartmouth, Canada
- Ishizaka J, Siswanto E, Itoh T, Murakami H, Yamaguchi Y, Horimoto N, Ishimaru T, Hashimoto S, Saino T (2007). Verification of vertically generalized production model and estimation of primary production in Sagami Bay, Japan. *J Oceanogr*, 63(3): 517–524
- Jin Z H, Charlock T P, Rutledge K, Stamnes K, Wang Y J (2006). Analytical solution of radiative transfer in the coupled atmosphere-ocean system with a rough surface. *Appl Opt*, 45(28): 7443–7455
- Jin Z H, Stamnes K (1994). Radiative transfer in nonuniformly refracting layered media: atmosphere-ocean system. *Appl Opt*, 33(3): 431–442
- Lee Z P (2009). KPAR: An optical property associated with ambiguous values. *Journal of Lake Sciences*, 21(2): 159–164
- Lee Z P, Carder K L, Marra J, Steward R G, Perry M J (1996). Estimating primary production at depth from remote sensing. *Appl Opt*, 35(3): 463–474
- Lee Z P, Du K P, Arnone R, Liew S C, Penta B (2005). Penetration of solar radiation in the upper ocean: a numerical model for oceanic and coastal waters. *J Geophys Res*, 110(C9): C09019
- Lee Z P, Weidemann A, Kindle J, Arnone R, Carder K L, Davis C (2007). Euphotic zone depth: Its derivation and implication to ocean-color remote sensing. *J Geophys Res*, 112(C3): C03009
- Li G (2006). Studies on the relationships of solar ultraviolet radiation (the UVR) and photosynthetic carbon fixation by phytoplankton assemblages from the South China Sea. Shantou: Shan Tou University (in Chinese)
- Li G, Che Z, Gao K S (2013). Photosynthetic carbon fixation by tropical coral reef phytoplankton assemblages: a the UVR perspective. *Algae*, 28(3): 281–288
- Li G, Gao K (2014). Effects of solar UV radiation on photosynthetic performance of the diatom *Skeletonema costatum* grown under nitrate limited condition. *Algae*, 29(1): 27–34
- Li G, Gao K S (2013). Cell size-dependent effects of solar UV on primary production in coastal waters of the South China Sea. *Estuaries Coasts*, 36(4): 728–736
- Li G, Gao K S, Gao G (2011). Differential impacts of solar UV radiation on photosynthetic carbon fixation from the coastal to offshore surface waters in the South China Sea. *Photochem Photobiol*, 87(2): 329–334
- Li G, Wu Y P, Gao K S (2009). Effects of typhoon Kaemi on coastal phytoplankton assemblages in the South China Sea, with special reference to the effects of solar UV radiation. *J Geophys Res*, 114 (G404029): 1–9
- Litchman E, Neale P J, Banaszak A T (2002). Increased sensitivity to ultraviolet radiation in nitrogen-limited dinoflagellates: photoprotection and repair. *Limnol Oceanogr*, 47(1): 86–94
- LokaBharathi P A, Krishnakumari L, Bhattathiri P M A, Chandramohan D (1997). UV radiation and primary production in the Antarctic waters. Scientific report: Thirteenth Indian Expedition to Antarctica, 323–334
- Lorenzen C J (1970). Surface chlorophyll as an index of the depth, chlorophyll content and primary productivity of the euphotic layer. *Limnol Oceanogr*, 15(3): 479–480
- Madronich S, McKenzie R L, Björn L O, Caldwell M M (1998). Changes in biologically active ultraviolet radiation reaching the earth's surface. *J Photochem Photobiol B*, 46(1–3): 5–19
- Marra J, Ho C, Trees C C (2003). An alternative algorithm for the calculation of primary productivity from remote sensing data. Lamont Doherty Earth Observatory Technical Report (LDEO-2003-1)
- Megard R O (1972). Phytoplankton, photosynthesis, and phosphorus in Lake Minnetonka, Minnesota. *Limnol Oceanogr*, 17(1): 68–87
- Mizubayashi K, Kuwahara V S, Segaran T C, Zaleha K, Effendy A W M, Kushairi MR M, Toda T (2013). Monsoon variability of ultraviolet radiation (the UVR) attenuation and bio-optical factors in the Asian tropical coral-reef waters. *Estuar Coast Shelf Sci*, 126: 34–43
- Neale P J, Cullen J J, Davis R F (1998). Inhibition of marine photosynthesis by ultraviolet radiation: variable sensitivity of phytoplankton in the Weddell-Scotia Confluence during the austral spring. *Limnol Oceanogr*, 43(3): 433–448
- Pang S H, Yu H F, He Y Y, Lv H X (2010). Response of Cyanobacterias to UV radiation. *Food Sci Technol (Campinas)*, 35(9): 41–45 (in Chinese)
- Singh J, Dubey A K, Singh R P (2011). Antarctic terrestrial ecosystem and role of pigments in enhanced UV-B radiations. *Rev Environ Sci Biotechnol*, 10(1): 63–77
- Smyth T J (2011). Penetration of UV irradiance into the global ocean. *J Geophys Res*, 116(C11): C11020
- Tanskanen A, Krotkov N A, Herman J R, Arola A (2006). Surface ultraviolet irradiance from OMI. *IEEE Trans Geosci Rem Sens*, 44 (5): 1267–1271
- Tedetti M, Sempéré R (2006). Penetration of ultraviolet radiation in the marine environment. A review. *Photochem Photobiol*, 82(2): 389–397
- Tedetti M, Sempéré R, Vasilkov A, Charrière B, Nérini D, Miller W L, Kawamura K, Raimbault P (2007). High penetration of ultraviolet radiation in the south east Pacific waters. *Geophys Res Lett*, 34(12): L12610
- Vasilkov A, Krotkov N, Herman J, McClain C, Arrigo K, Robinson W (2001). Global mapping of underwater UV irradiances and DNA-weighted exposures sea-viewing using total ozone mapping spectrometer and wide field-of-view sensor data products. *J Geophys Res*, 106(C11): 27205–27219
- Vasilkov A P, Herman J R, Ahmad Z, Kahru M, Mitchell B G (2005). Assessment of the ultraviolet radiation field in ocean waters from space-based measurements and full radiative-transfer calculations. *Appl Opt*, 44(14): 2863–2869
- Villafañe V E, Sundbäck K, Figueroa F L, Helbling E W (2003).

- 1 Photosynthesis in the aquatic environment as affected by UVR. UV effects in aquatic organisms and ecosystems. The Royal Society of Chemistry, Cambridge: 357–397
- 5 Vincent W F, Roy S (1993). Solar ultraviolet-B radiation and aquatic primary production: damage, protection, and recovery. *Environ Rev*, 1(1): 1–12
- 10 Wang P C, Wu B Y, Zhang W X (1999). Comparison of UV simulation and measurements of surface ultraviolet radiation. *Chinese Journal of Atmosphere Sciences*, 23(3): 359–364 (in Chinese)
- 15 Wang Y, Yang Z, Tang X X, Liu Y, Li Y Q (2002). The sensitivity variability of seven species of marine microalgae to the influence of UV-B radiation. *Acta Scientiae Circumstantiae*, 22(2): 225–230 (in Chinese)
- 20 Wu Y P, Gao K S (2011). Photosynthetic response of surface water phytoplankton assemblages to different wavebands of UV radiation in the South China Sea. *Acta Oceanol Sin*, 33(5): 146–151 (in Chinese)
- 25 Wu Y P, Gao K S, Li G, Helbling E W (2010). Seasonal impacts of solar UV radiation on photosynthesis of phytoplankton assemblages in the coastal waters of the South China Sea. *Photochem Photobiol*, 86(3): 586–592
- 30 Yuan X C, Yin K D, Zhou W H, Cao W X, Xu X Q, Zhao D (2007). Effects of ultraviolet radiation B (UV-B) on photosynthesis of natural phytoplankton assemblages in a marine bay in Southern China. *Chin Sci Bull*, 52(4): 545–552
- 35 Zhang P Y, Tang X X, Cai P J, Yu J, Yang Z (2005). Effects of UV-B radiation on protein and nucleic acid synthesis in three species of marine Red-Tide Microalgae. *Acta Phytoecol Sin*, 29(3): 505–509 (in Chinese)
- 40
- 45
- 50
- 55